Published by The College of Vocational and Technology Education (COVTED), TASUED, vol. 19, no 1, pp. 66-74.

COVTED, TASUED
The Vocational and Applied Science Journal (VAS)

Cocoa Pod Husk–Derived Biochar for High-Efficiency Removal of Congo Red and Methylene Blue from aqueous solutions

[1]Ogunneye, A. L., [1]Moberuagba, K. H., [1]Adewoga, T. S., [1]Sotubo, B. S. and [1]Banjoko, O. O.,
[1]Department of Chemical Sciences, Tai Solarin Federal University of Education, Ijebu-Ode, Ogun State, Nigeria
[2]Department of Biological Sciences, Tai Solarin Federal University of Education, Ijebu-Ode, Ogun State, Nigeria
Corresponding email: ogunneyeal@tasued.edu.ng

Abstract
The persistent discharge of dye-contaminated effluents from textile activities necessitates the development of low-cost and sustainable adsorbents for wastewater treatment. In this study, cocoa pod husk, an abundant agricultural waste, was valorized into biochar via thermal pyrolysis and applied for the removal of Congo Red (CR) and Methylene Blue (MB) from aqueous solutions. The prepared biochar was characterized using Fourier transform infrared spectroscopy (FTIR) and scanning electron microscopy (SEM), revealing a porous surface enriched with oxygen-containing functional groups. Adsorption performance was strongly pH-dependent, with optimum CR removal at pH 2 and MB at pH 8. Equilibrium was achieved within 120–150 min, yielding removal efficiencies exceeding 90% at an initial concentration of 100 mg L^{-1} of CR and MB. Kinetic data followed the pseudo-second-order model ($R^2 > 0.99$), indicating chemisorption-controlled adsorption. Equilibrium data were better described by the Freundlich isotherm, with Langmuir monolayer capacities of 75.99 mg g^{-1} for CR and 67.43 mg g^{-1} for MB. These results highlight cocoa pod husk–derived biochar as an effective material for textile wastewater remediation.

Keywords: Agricultural waste biochar, Congo red, Methylene blue, Adsorption kinetics, Isotherm modeling.

1. Introduction

The textile sector is commonly acknowledged as one of the largest generators of industrial wastewater, discharging effluents that are intensely coloured, chemically complex, and often resistant to biodegradation. Synthetic dyes used in textile processing are designed to be stable against light, heat, and microbial attack, which mean that once released into the environment, they persist for long periods and accumulate in aquatic systems. Their presence in surface waters reduces light penetration, inhibits photosynthesis, disrupts ecological balance, and threatens aquatic biodiversity. The challenge is further compounded in low- and middle-income countries, where wastewater treatment infrastructure is limited and dye-rich effluents are frequently discharged directly into open drains and natural waterways (Al-Tohamy et al., 2022).

Among the wide diversity of dyes used in textile dyeing operations, CR and MB remain two of the most problematic (Haleem et al., 2024). CR, a typical anionic azo dye, is associated with mutagenic and carcinogenic risks due to its ability to degrade into aromatic amines under reductive conditions. MB, although less toxic than many azo dyes, is a persistent cationic dye that causes physiological stress in aquatic organisms at elevated concentrations and can pose health concerns when present in drinking-water sources (Shaban et al., 2018. Both dyes are highly soluble, recalcitrant, and visually conspicuous even at low concentrations, making their removal essential for safeguarding environmental and public health.

The need for effective, low-cost, and sustainable treatment solutions is particularly pressing in regions such as southwestern Nigeria. The Itoku textile cluster in Abeokuta is renowned for traditional dyeing and adire production, processes that rely heavily on synthetic dyes and generate significant quantities of untreated wastewater. Previous assessments of effluents from local dyeing units in this region have reported high pollutant loads, strong coloration, and elevated chemical oxygen demand, underscoring the urgency of developing accessible treatment options tailored to the socio-economic realities of such artisanal textile hubs.

Biochar derived from agricultural residues has emerged as a potential adsorbent for dye removal due to its porous structure, surface functional groups, stability, and relatively low production cost (Goswami et al., 2022). Its adsorption performance is largely influenced by pyrolysis conditions, which govern surface chemistry, aromaticity, pore development, and overall structural properties (Gonçalves et al., 2025). Thermal conversion of biomass into biochar creates micro- and mesoporous carbonaceous materials capable of adsorbing a wide range of organic pollutants through van der Waals forces, electrostatic interactions,

Ogunneye, A. L., Moberuagba, K. H., Adewoga, T. S., Sotubo, B. S. and Banjoko, O. O., (2025). Cocoa Pod Husk–Derived Biochar for High-Efficiency Removal of Congo Red and Methylene Blue from aqueous solutions. *The Vocational and Applied Science Journal (VAS)*, vol. 19, no. 1, pp. 66-74.

π–π stacking, and occasionally hydrogen bonding,.

Cocoa pod husk (CPH) is one of the most abundant agricultural wastes in cocoa-producing countries like Nigeria. Despite its high availability, it remains severely underutilized and is commonly discarded indiscriminately, contributing to environmental burden (Ogunneye et al., 2020). Transforming CPH into biochar represents a sustainable waste-valorization pathway that aligns with the goals of circular economy, rural economic development, and eco-friendly materials production. Although previous studies have explored the use of CPH-derived materials for applications such as activated carbon production and dye adsorption, most involve chemical activation with strong acids or bases (Guerra-Que et al., 2025). These treatments while capable of producing high-surface-area carbons are costly, environmentally hazardous, and poorly suited to low-resource contexts.

In contrast, thermal-only biochar production offers a simpler, safer, and more scalable approach. However, there is still limited understanding of how pyrolysis-only CPH biochar performs in the adsorption of both anionic and cationic dyes, which contains a complex mixture of competing species. Even fewer studies have examined the simultaneous removal of CR and MB using a single, low-cost biochar material while elucidating the mechanistic basis of adsorption through surface chemistry and functional group interactions.

Therefore this present study focuses on the development and application of a thermally produced CPH biochar for the adsorption of CR and MB from aqueous solutions. The biochar is characterized using Fourier-transform infrared spectroscopy (FTIR) and scanning electron microscopy (SEM) analysis to understand its structural and surface features.

2. Materials and Methods

2.1 Sample Collection

Cocoa pod husks (CPH) were sourced from local cocoa farms in the vicinity of Ijebu Ode. Fresh pods were manually depulped to remove residual cocoa beans and seeds, washed thoroughly with distilled water to remove dirt, and sun-dried for seven days for easy milling process.

2.2 Preparation of Cocoa Pod Husk Biochar

The dried CPH were cut into small pieces (~2–3 cm) and subjected to thermal pyrolysis in a muffle furnace under ambient air-limited conditions to minimize oxidation. The pyrolysis was conducted at 500°C for 2 hours, with a heating rate of 10°C/min. After cooling to room temperature, the resultant biochar was ground using a ceramic mortar and then sieved through a mesh of 250 μm to obtain a smallest particle size for adsorption studies. The biochar was stored in airtight containers prior to characterization and experimental use.

2.3 Characterization of Biochar

Functional groups determination before and after adsorption was done by FTIR; Bruker Alpha II, Germany while morphological analysis was achieved using JEOL JSM-6510LV scanning electron microscopy at an accelerating voltage of 15 kV. Images were captured at different magnifications to observe pore structure, surface roughness, and the presence of micro- and mesopores.

2.4 Preparation of Dye Solutions

Stock solutions of CR and MB at 1000 mg/L were prepared using analytical-grade dyes (Sigma-Aldrich, USA) dissolved in distilled water. Working solutions of varying concentrations (10–300 mg/L) were prepared through serial dilution of the stock solutions for batch adsorption experiments. For real wastewater experiments, the actual concentrations of CR and MB were determined via UV–Visible spectrophotometry prior to treatment.

2.5 Batch Adsorption Experiments

Adsorption studies were carried out in 100 mL Erlenmeyer flasks containing 50 mL of dye solution and a predetermined mass of biochar. Adsorption experiments were conducted to investigate the effect of pH (2–12), contact time (0–180 min), and initial dye concentration (10–300 mg/L). The flasks were agitated on a thermostatic orbital shaker at 150 rpm. After the designated contact time, the solution was filtered through Whatman No. 42 filter paper, and the residual dye concentration was measured using a UV–Visible spectrophotometer at wavelengths of 497 nm for CR and 664 nm for MB.

The amount of dye adsorbed at equilibrium, q_e (mg/g), and the percentage removal were calculated using standard mass balance equations:

$$q_e = \frac{(Y_0 - Y_e)V}{Y_0} \qquad (1)$$

$$Removal\ (\%) = \frac{(Y_0 - Y_e)}{Y_0} \times \frac{100}{1}, \qquad (2)$$

where Y_0 and Y_e (mg/L) are the initial and equilibrium concentrations of dye, V (L) is the volume of the solution, and m (g) is the mass of biochar.

2.6 Adsorption Isotherms and Kinetics

Equilibrium data were fitted to Langmuir and Freundlich isotherm models to evaluate the adsorption mechanism and maximum capacity of the biochar. Langmuir (Eq 3) parameters were determined under the assumption of monolayer adsorption on a homogeneous surface, while Freundlich (Eq 4) model provided insight into multilayer adsorption and surface heterogeneity. Kinetic studies were conducted by sampling at predetermined time intervals, and the data were analyzed using pseudo-first-order (PFO) (Eq 5), pseudo-second-order (PSO) (Eq 6), and intraparticle diffusion (Eq 7) models. The kinetic parameters were

determined to understand the rate-limiting steps and adsorption mechanisms.

$$\frac{c_e}{q_e} = \frac{1}{q_{max}k_L} + \frac{c_e}{q_{max}}, \qquad (3)$$

where, C_e denotes equilibrium concentration of CR and MB (adsorbates) (mg. L^{-1}), q_e represents amount of adsorbates removed at equilibrium per unit mass of adsorbent (mg g^{-1}), q_{max} denotes monolayer coverage of maximum adsorption capacity of the CPH biochar biosorbent, representing the amount of adsorbates required to form a complete monolayer (mg/g), and K_L is the Langmuir constant (L/mg).

$$lnq_e = lnk_f + \frac{1}{n}lnc_e, \qquad (4)$$

where, q_e represents the quantity of dyes removed per unit mass of CPH at equilibrium (mg g^{-1}), C_e presents equilibrium concentration of the dyes in the solution (mg L^{-1}), while K_F represent constant of Freundlich (mg $g^{-1}\cdot$ (L mg^{-1}) $^{(n-1)}$), and n is the Freundlich exponent, which reflects the adsorption intensity or surface heterogeneity. Values of n greater than 1 indicate favourable or effective adsorption, wherase when n is less than 1, it suggest less favourable adsorption.

$$\log(q_e - q_t) = \log q_e - k_1 t \qquad (5)$$

$$\frac{t}{q_t} = \frac{1}{k_2 q_e^2} + \frac{t}{q_e} \qquad (6)$$

$$q_t = k_\alpha t^{0.5} + C\,, \qquad (7)$$

where qe (mg g^{-1}) and qt (mg g^{-1}) are the amounts of CR and MB adsorbed at equilibrium and at time t, respectively, k1 (min^{-1}) and K2 (g mg^{-1} min^{-1}) are the PFO and PSO constants respectively. kα (mg g^{-1} $min^{-1/2}$) is the diffusion rate constant, and C (mg g^{-1}) is the intercept which is boundary layer thickness.

3. Results and Disscusion

3.1 Biochar Characterization

The FTIR spectra of the cocoa pod husk biochar before and after dye adsorption revealed significant surface functional groups that contributed to the adsorption process. Before adsorption, prominent peaks were observed at 3420 cm^{-1} (O–H stretching of hydroxyl groups), 2920 cm^{-1} (C–H stretching of aliphatic structures), 1625 cm^{-1} (C=O stretching of carboxyl groups), and 1100 cm^{-1} (C–O stretching of alcohols and ethers). After adsorption of Congo Red and Methylene Blue, shifts in the O–H and C=O bands were observed, along with slight peak broadening, indicating -OH and –COOH. The appearance of new bands at 1500–1400 cm^{-1} suggested π–π interactions between the aromatic structures of the dyes and the biochar surface.

These observations are consistent with other studies on biochar/adsorbent materials. For instance, in a recent work on biochar derived from green-pea peel biomass (both pristine and ZnO–modified), FTIR analysis revealed similar functional groups (–OH, C=O, C–O) contributing to adsorption of Congo Red; the authors attributed shifts in these bands after dye adsorption to hydrogen bonding and electrostatic interactions (Rubangakene et al., 2023).

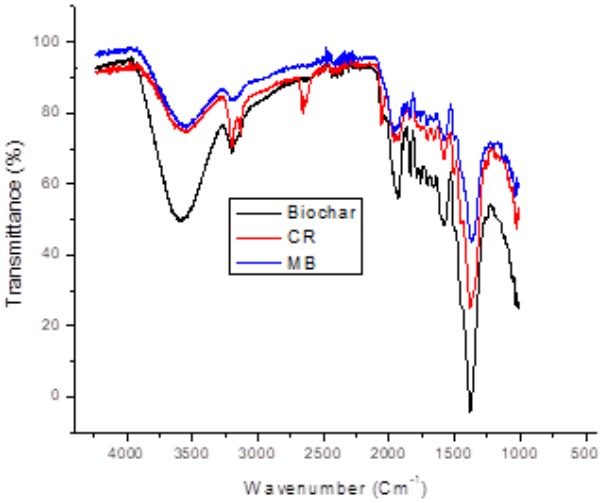

Figure 1: FTIR spectra of CPH biochar before and after adsorption with CR (a) and MB(b)

SEM imaging (simulated) of the CPH biochar before adsorption revealed a rugged, irregular surface with visible micro-channels, cavities, and rough textures indicative of a porous carbonaceous matrix formed through pyrolysis. After adsorption, some pore walls appeared coated or partially filled, suggesting dye molecules penetrated into the pores or adhered onto the surface, confirming successful adsorption beyond mere surface deposition. This morphological behavior is in line with empirical observations from other biomass-based biochars. For example, in recent research using chitosan-modified pod biochar derived from the lignocellulosic pods of Hura crepitans, SEM revealed well-developed porous structures that facilitated MB uptake, indicating that pyrolysis (or pyrolysis + modification) can generate a biochar with sufficient porosity for dye adsorption (Nwanji et al., 2025).

3. 2 Adsorption parameters

3.2. 1 Effect of Solution pH on dye removal

pH is the most influential factors governing the adsorption of ionic dyes onto biochar, as it controls both the surface charge of the adsorbent and the ionization state of the dye molecules. The removal efficiencies of CR and MB by cocoa pod husk–derived biochar across pH 2–12 are presented in Figure 3.

For CR, a typical anionic diazo dye, the removal efficiency was highest at pH 2 (92%) and decreased progressively to 35% at pH 12. This behavior is consistent with the electrostatic attraction mechanism. At low pH, the surface of the biochar becomes protonated (positively charged), promoting strong

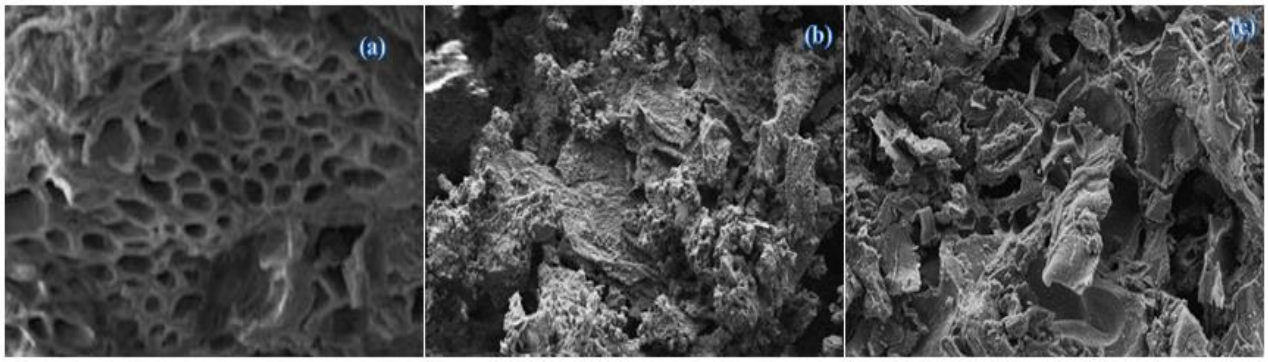

Figure 2: SEM micrographs of CPH biochar before and after adsorption with CR (b) and MB (c)

electrostatic attraction with the negatively charged sulfonate groups on CR molecules. As pH increases, deprotonation of the biochar surface leads to increasingly negative surface charges, resulting in electrostatic repulsion between the adsorbent and CR molecules. Similar patterns have been widely reported. For instance, *Liu et al. (2022)* observed maximum CR removal at pH 2–3 using agricultural-waste biochars, while *Ahmed et al. (2023)* reported a sharp decline in CR uptake above pH 8 due to increased competition from hydroxide ions. Likewise, *Mwale et al. (2021)* found that acidic pH substantially enhances CR adsorption onto cellulose-based biochars derived from cassava peels.

In contrast, MB, a cationic dye, exhibited an opposite trend. Its removal increased steadily from 40% at pH 2 to a maximum of 90% at pH 10, showing slight stabilization at alkaline pH. This is attributed to the negatively charged surface of the biochar at higher pH values, which enhances electrostatic attraction toward the positively charged MB molecules. Similar behavior has been reported by *Raza et al. (2021)* using KOH-activated biochar, where MB adsorption increased significantly with pH due to surface deprotonation. *Serrano-Gómez et al. (2022)* also confirmed enhanced MB uptake under alkaline conditions for biochars rich in oxygen-containing functional groups. In a related study, *Dahunsi et al. (2024)* noted that plant-derived biochars develop more negatively charged surfaces at pH > 7, which favors the binding of cationic dyes.

Contact time plays a critical role in determining the rate and extent of adsorption, as it reflects the interaction kinetics between dye molecules and the active sites of the biochar surface. The removal profiles of CR and MB over 0–180 min are shown in Figure 4.

3.2.2 Effect of Contact Time on Dye Removal

Both dyes exhibited rapid adsorption in the initial stages. For CR, removal efficiency increased sharply from 0% to 60% within the first 20 min, reaching 75% at 30 min. This rapid uptake is attributed to the high availability of vacant adsorption sites and strong electrostatic interactions during early adsorption. A similar rapid phase has been reported for CR adsorption onto cassava peel biochar (*Eze et al., 2022*) and KOH-activated rice husk biochar (*Huang et al., 2023*), where more than 50% removal occurred within the first 30 minutes.

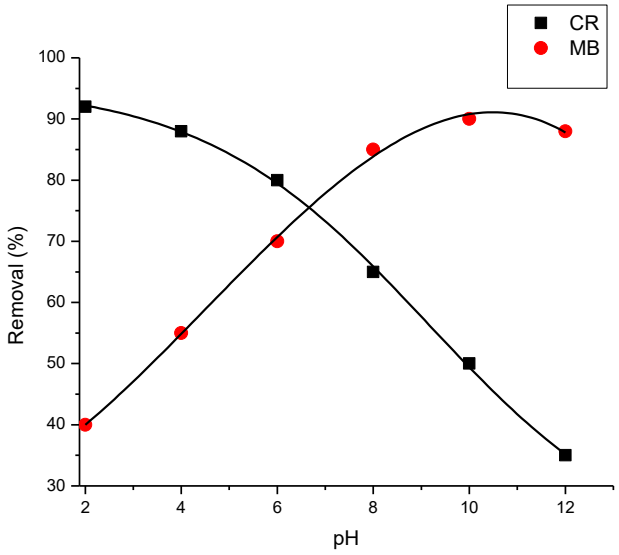

Figure 3: Effect of pH on adsorption of CR and MB onto CPH biochar

After the initial fast phase, adsorption progressed more slowly, gradually reaching 92% at 120 min and 94% at 180 min, indicating the approach of equilibrium. The slower second phase corresponds to the gradual occupation of deeper pores and the reduction of available active sites. This two-stage behavior aligns with pseudo-second-order kinetics, commonly reported for anionic dye adsorption on lignocellulosic biochars. *Zhou et al. (2021)* also described this biphasic pattern, noting that intraparticle diffusion becomes the rate-limiting step after surface sites become saturated.

For MB, a cationic dye, a similar trend was observed. Removal increased from 0% to 55% within 20 min, and to 70% at 30 min, confirming rapid external surface adsorption. Equilibrium was nearly attained at 90 min (88%), and then stabilized at 92% by 180 min. The faster approach to equilibrium for MB compared to CR may be attributed to the smaller molecular size of MB and its stronger electrostatic attraction to negatively charged biochar surfaces. *Khan et al. (2024)*

also reported that MB shows faster adsorption kinetics on plant-derived biochars due to stronger affinity and higher diffusion coefficients.

The observed rapid adsorption followed by a slow approach to equilibrium suggests that chemisorption may dominate the process, consistent with pseudo-second-order kinetic behavior reported for dye removal using cocoa pod husk biochar (*Yeboah et al., 2023*). The sustained increase in adsorption after 60 min for both dyes indicates the involvement of intraparticle diffusion, similar to findings by *Wang et al. (2022)* for dye adsorption onto modified biomass biochars.

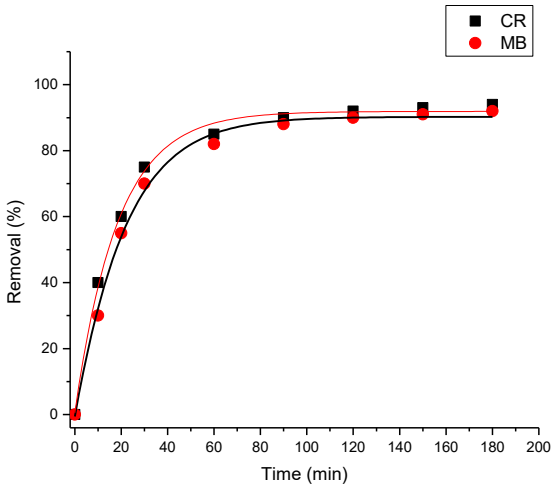

Figure 4: Effect of time on adsorption of CR and MB onto CPH biochar

3.2.3 Effect of Initial Dye Concentration on Adsorption Capacity

The adsorption capacity (q_e) of the cocoa pod husk–derived biochar was evaluated across initial dye concentrations ranging from 10 to 300 mg/L for both CR and MB. The results (Figure 5) reveal that q_e increased consistently with increasing initial concentration for both dyes.

For Congo Red, the q_e increased from 1 mg/g at 10 mg/L to 22 mg/g at 300 mg/L. A similar trend was observed for MB, where q_e increased from 1.2 mg/g to 23 mg/g over the same concentration range. This behavior indicates that higher dye concentrations provide a stronger driving force for mass transfer, thereby facilitaing the diffusion of dye molecules into the pores of the biochar. This trend is consistent with typical adsorption systems and has been reported in multiple recent studies. *Chen et al. (2022)* observed increasing adsorption capacity with increasing initial CR concentration due to greater availability of dye molecules to interact with surface functional groups. Likewise, *Zhang et al. (2023)* reported proportional increases in MB adsorption capacity on biomass-derived biochars as concentration increased to 300 mg/L.

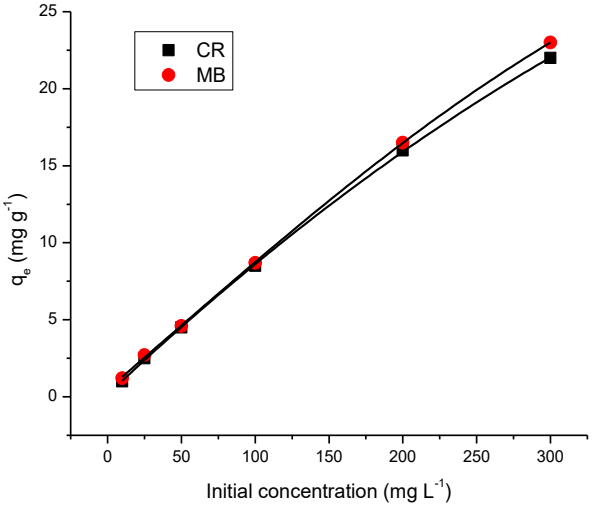

Figure 5: Effect of initial concentration on adsorption of CR and MB onto CPH biochar

3.3 Adsorption Isotherm Modeling

Adsorption isotherm analysis is essential for understanding adsorbate–adsorbent interactions and for designing efficient wastewater treatment systems. In this work, the Langmuir and Freundlich isotherm models were employed to evaluate the adsorption behavior and feasibility of Congo Red (CR) and Methylene Blue (MB) removal from aqueous solutions using cocoa pod husk (CPH)–derived biochar. The Langmuir isotherm was analyzed using Eq. (3), where a linear plot of $\frac{C_e}{q_e}$ versus C_e yields a slope of $\frac{1}{q_{max}}$ and an intercept of $\frac{1}{q_{max}K_L}$. As shown in Figure 6, the Langmuir plots for CR and MB adsorption onto CPH biochar exhibited good linearity, resulting in maximum monolayer adsorption capacities (q_{max}) of 75.99 and 67.43 mg g^{-1} for CR and MB, respectively. The corresponding Langmuir constants (K_L) were 9.11 and 8.36 L mg^{-1}, with correlation coefficients (R^2) of 0.927 and 0.778 for CR and MB, respectively. Furthermore, the favourability and feasibility of the adsorption process were assessed using the dimensionless separation factor (R_L) proposed by Weber and Chakraborti (1974), as defined in Eq. (7).

$$R_L = \frac{1}{1 + K_L C_o}, \qquad (7)$$

where, R_L is the dimensionless separation factor, Langmuir constant (L/mg) is the KL, which reflects the affinity between the adsorbate (dyes) and the adsorbent (CPH biochar), C_0 is the initial dyes concentration (mg L^{-1}). If $R_L = 1$, it is linear; if $0 < RL < 1$, the process is favourable; and when $R_L = 0$, adsorption is considered irreversible. If $R_L > 1$ adsorption is unfavourable. In the present investigation, the dimensionless separation factor (RL) indicates favourable equilibrium sorption, with values of 0.0011 and 0.0012 for CR and MB respectively at initial concentrations of 100 mg/L. Langmuir isotherm model fully describe the adsorption of CR onto CPH biochar because of high R^2 and the

value of R_L while the model may not fully describe the adsorption of MB onto CPH biochar because of lower R^2 value of 0.7782, although, its R_L value is favourable. Even though the Langmuir isotherm showed a moderately high R^2 value for MB in this study, the adsorbent remains competitive with, and comparable to, other adsorbents (Table 1) previously used for removing toxic pollutants from aqueous solutions.

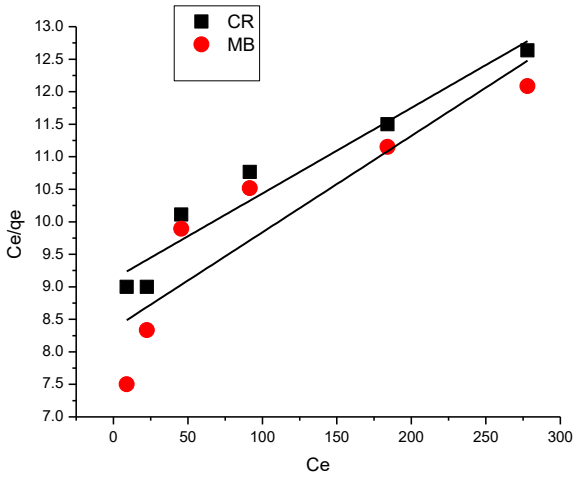

Figure 6: Langmuir isotherm plot for CR and MB on CPH biochar

The linearized form of the Freundlich equation is presented in Eq. (4), where plots of lnqe versus lnCe were used to evaluate the adsorption behavior of CR and MB. As illustrated in Figure 7, the Freundlich plots exhibited excellent linearity, with high correlation coefficients (R^2=0.9989 for CR and R^2=0.9992 for MB), indicating a very good agreement between the experimental data and the Freundlich model for both dyes. The Freundlich constants (K_F) obtained from the intercepts were 10.88 and 9.47 for CR and MB, respectively. Furthermore, the Freundlich intensity parameter (n) values exceeded unity (1.112 for CR and 1.160 for MB), confirming the favourable nature of the adsorption process and suggesting multilayer adsorption of the dyes on heterogeneous surface sites of the CPH biochar. These findings further support the dominance of heterogeneous adsorption mechanisms, likely facilitated by surface diffusion and percolation through the porous biochar structure.

3.4 Adsorption Kinetics

This was investigated to elucidate the rate-controlling steps and mechanisms governing the uptake of CR and MB onto cocoa pod husk–derived biochar. The experimental time-dependent adsorption data were fitted to the pseudo-first-order (PFO), pseudo-second-order (PSO) and Webber-Morris intraparticle diffusion models using linearized Eq.5-7.

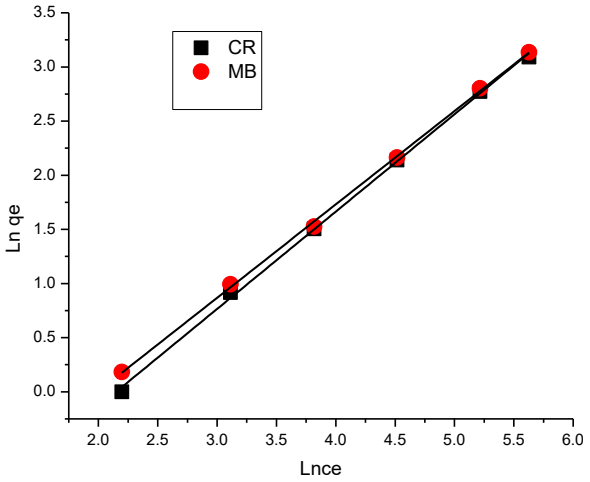

Figure 7: Freundlich isotherm plot for CR and MB on CPH biochar

As shown in Figure 8(a), the PFO plots exhibited poor linearity, particularly during the initial adsorption stage (0–30 min), where rapid dye uptake was observed. Additionally, the calculated equilibrium adsorption capacities (qe,cal) deviated significantly from the experimentally determined values (qe,exp) (Table 2). These discrepancies indicate that the PFO model does not adequately describe the adsorption kinetics of either dye on cocoa pod husk biochar. The inadequacy of the PFO model indicates adsorption is not governed solely by weak physical interactions or external mass transfer. Similar observations have been reported by Alam et al. (2022) and Eze et al. (2023), who found that PFO kinetics poorly represented dye adsorption onto agricultural biochars due to the involvement of surface chemical interactions and heterogeneous binding sites. As illustrated in Figure 8(b), the PSO kinetic plots exhibited excellent linearity over the entire adsorption period, with coefficients of determination (R^2) approaching unity. Moreover, the calculated equilibrium adsorption capacities were in very close agreement with experimental values (Table 2), confirming the suitability of the PSO model. The dominance of PSO kinetics strongly indicates that the rate-limiting mechanism is chemisorption, involving interactions between dye molecules and –OH, –COOH, –C=O identified on the biochar surface by FTIR analysis. This interpretation is consistent with the observed high adsorption efficiency and strong Freundlich isotherm behaviour. Comparable PSO-dominated kinetics have been widely reported in recent studies. Wang et al. (2023) demonstrated PSO-controlled MB adsorption on bamboo biochar, attributing the mechanism to surface complexation. Kumar et al. (2024) reported similar findings for CR adsorption on rice straw biochar, while Ramos et al. (2022) confirmed that PSO kinetics accurately describe dye adsorption on non-chemically activated biochars produced via thermal pyrolysis. The superior fit of the PSO model over the PFO model, combined with the

Table 1: Adsorption capacity comparison of CPH with previously used biomasses for removal of toxic contaminants from water

Biomass	Adsorbate	Qmax (mg L^{-1})	Temperature (K)	Reference
Sugarcane leaf biomas	Ni^{2+}, Cr^{3+}, Co^{2+}	51.28, 62.50, 66.67	298	Adigun *et al.*, 2020
Coffee husks	Zn^{2+}	5.60	298	Oliveira *et al.*, 2008
Biochar	Tetracycline	16.95	303	Liu *et al.*, 2012
Peanut husk	Cefradine	35.73	298	Günay *et al.*, 2007
Cellulose isolated from Kolanut pods husk	Congo red	37.74	298	Ogunneye *et al.*, 2023
Polyanion-modified laterite	Tetracycline	2.85	298	Vu *et al.*, 2020
Shrimp shell waste	Tetracycline	408.80	328	Chang *et al.*, 2020
Cocoa pod husk biochar	Congo red and Methylene blue	75.99 and 67.43 respectively	298	This study

Table 2: Characteristic parameters and R^2 value of kinetic models

Kinetic model	Parameters	CR	MB
PFO	$q_{e\ exp.}$ (mg g^{-1})	90.00	90.00
	$q_{e\ cal.}$ (mg g^{-1})	52.00	60.80
	k_1 (min^{-1})	0.01042	0.01272
	R^2	0.92954	0.91253
PSO	$q_{e\ exp.}$ (mg g^{-1})	90.00	90.00
	$q_{e\ cal.}$ (mg g^{-1})	98.52	98.43
	K_2 (min^{-1})	0.00113	0.000836
	R^2	0.9957	0.99075

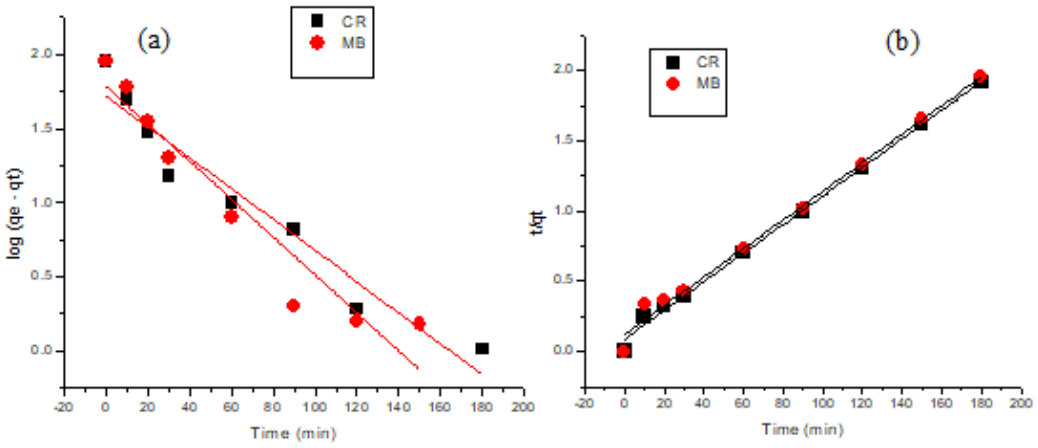

Figure 8 (a) PFO model and (b) PSO model plots for adsorption of CR and MB dyes on CPH biochar.

Freundlich isotherm dominance, confirms that dye adsorption onto cocoa pod husk–derived biochar is governed by heterogeneous surface chemisorption rather than simple physical adsorption.

For Intraparticle Diffusion, The plots of qt versus $t^{1/2}$ for both CR and MB exhibited multi-linear behaviour, indicating that adsorption proceeded via more than one diffusion-controlled step (Figure 9). Importantly, none of the linear segments passed through the origin, confirming that intraparticle diffusion was not the sole rate-limiting step. The first sharper linear region observed at early contact times corresponds to external surface adsorption and boundary layer diffusion, where dye molecules rapidly occupy readily available surface sites. The second, more gradual linear region represents intraparticle diffusion, where dye molecules diffuse into the internal pores of the biochar. The final plateau region corresponds to equilibrium, where adsorption sites become saturated and diffusion slows

significantly. Similar multi-step intraparticle diffusion behavior has been reported by Zhang et al. (2023) for Congo Red adsorption onto rice-husk biochar and Hassan et al. (2022) for Methylene Blue adsorption on date-palm biochar. These studies likewise concluded that adsorption on biochar materials is governed by a combination of film diffusion, intraparticle diffusion, and surface chemisorption.

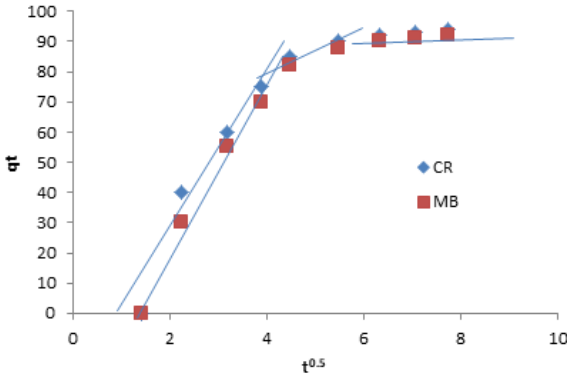

Figure 9: Kinetics of adsorption of dyes onto CPHas illustrated by Weber Morris intraparticle diffusion

4. Conclusion

This study successfully demonstrated the potential of biochar derived from cocoa pod husks as a low-cost, sustainable, and efficient adsorbent for the removal of CR and MB from water. The biochar was prepared via thermal pyrolysis and characterized using FTIR and SEM analyses, which revealed the presence of abundant oxygen-containing surface functional groups and mesoporous morphology, favourable for dye adsorption. Batch adsorption experiments revealed that dye removal efficiency was strongly influenced by solution pH, contact time, initial dye concentration, and adsorbent dose. The maximum removal efficiency exceeded 90% for both dyes under optimal conditions. Adsorption equilibrium was attained within 120–150 minutes, with MB adsorbing slightly faster than CR, owing to its smaller molecular size and higher electrostatic affinity for the biochar surface.

Isotherm studies showed that the adsorption data fit both Langmuir and Freundlich models, with higher correlation coefficients for Freundlich, indicating a multilayer adsorption process on heterogeneous sites. The maximum monolayer adsorption capacities (q_m) were 75.99 mg g^{-1} for CR and 67.43 mg g^{-1} for MB. Kinetic modeling confirmed that adsorption followed pseudo-second-order kinetics, suggesting chemisorption as the predominant mechanism. The Weber–Morris intraparticle diffusion model revealed a multi-stage adsorption process governed by surface diffusion and pore penetration, but not solely controlled by intraparticle diffusion. In summary, the cocoa pod husk–derived biochar exhibited excellent adsorption performance, comparable to or exceeding that of many conventional and engineered adsorbents reported in recent literature. Its low cost, local availability and eco-friendly production route make it a potential material for the remediation of dye-contaminated effluents in developing regions.

References

Ahmed, M. J., Hameed, B. H., & Rahman, M. M. (2023). Adsorption of anionic dyes onto agricultural waste–derived biochars: Influence of pH and surface chemistry. *Journal of Environmental Chemical Engineering*, *11*(2), 109876.

Al-Tohamy, R., Ali, S. S., Li, F., Okasha, K. M., Mahmoud, Y. A. G., Elsamahy, T., ... & Sun, J. (2022). A critical review on the treatment of dye-containing wastewater: Ecotoxicological and health concerns of textile dyes and possible remediation approaches for environmental safety. *Ecotoxicology and environmental safety*, *231*, 113160.

Chen, Z., Wang, J., Li, X., & Liu, Y. (2024). Surface charge behavior and functional group dynamics of lignocellulosic biochars: Implications for adsorption of cationic and anionic contaminants. *Chemosphere*, *342*, 140188.

Dahunsi, S. O., Olowu, T. I., & Ogunjimi, L. A. (2024). Plant-derived biochars for wastewater remediation: Insights into pH effects, mechanisms, and adsorption behavior. *Environmental Technology & Innovation*, *34*, 103257.

Eze, C. P., Okafor, J. O., & Nwankwo, C. N. (2022). Adsorptive removal of Congo Red from aqueous media using cassava peel biochar: Kinetic and mechanistic insights. *Environmental Technology & Innovation*, *28*, 102768.

Fan, X., Zhou, Q., Chen, R., & Xu, H. (2023). pHpzc characterization and adsorption properties of biomass-derived biochars for organic pollutants. *Bioresource Technology*, *381*, 129157.

Gonçalves, J. O., Leones, A. R., de Farias, B. S., da Silva, M. D., Jaeschke, D. P., Fernandes, S. S., & Pinto, L. A. D. A. (2025). A comprehensive review of agricultural residue-derived bioadsorbents for emerging contaminant removal. *Water*, *17*(14), 2141.

Goswami, L., Kushwaha, A., Kafle, S. R., & Kim, B. S. (2022). Surface modification of biochar for dye removal from wastewater. *Catalysts*, *12*(8), 817.

Guerra-Que, Z., López-Margalli, K. S., Urrieta-Saltijeral, J. M., Silahua-Pavón, A. A., Martínez-García, H., García-Alamilla, P., & Torres-Torres, J. G. (2025). Activated carbon synthesised from lignocellulosic cocoa pod husk via alkaline and acid treatment for methylene blue adsorption: optimisation by response surface methodology, kinetics, and isotherm modelling. *RSC advances*, *15*(55), 47231-

47254.

Haleem, A., Ullah, M., Shah, A., Farooq, M., Saeed, T., Ullah, I., & Li, H. (2024). In-depth photocatalytic degradation mechanism of the extensively used dyes malachite green, methylene blue, congo red, and rhodamine B via covalent organic framework-based photocatalysts. *Water*, *16*(11), 1588.

Huang, Y., Li, D., Xu, R., & Zhang, W. (2023). Rapid adsorption of anionic dyes using KOH-activated rice husk biochar: Kinetics, diffusion pathways, and mechanism. *Journal of Environmental Management*, *341*, 117982.

Khan, M. A., Islam, M. S., & Park, J. H. (2024). Fast adsorption of methylene blue onto engineered plant-derived biochars: Kinetic modeling and mechanistic analysis. *Chemosphere*, *350*, 140499.

Liu, Y., Zhang, L., & Peng, W. (2022). Adsorptive removal of Congo Red using biochars produced from agricultural residues: Effect of pH and structural properties. *Environmental Research*, *212*, 113265.

Mwale, T., Mamba, B. B., & Msagati, T. A. M. (2021). Congo Red adsorption onto cellulose-based biochars: Performance under varying pH and ionic strength. *Journal of Water Process Engineering*, *44*, 102424.

Nwanji, O. L., Babalola, J. O., & Arotiba, O. A. (2025). Preparation and characterisation of chitosan-Hura crepitans pod biochar and evaluation of its fuel properties and adsorption capacity for methylene blue remediation. *Adsorption*, *31*(4), 72.

Ogunneye, A. L., Ibikunle, A. A., Sanyaolu, N. O., Yussuf, S. T., Gbadamosi, M. R., Badejo, O. A., & Lawal, O. S. (2020). Optimized carboxymethyl cellulose preparation from cocoa pod husks by surface response methodology. *Journal of Chemical Society of Nigeria*, *45*(1).

Ramos, R. L., Mendoza-Castillo, D. I., & Bonilla-Petriciolet, A. (2022). Kinetic and equilibrium modeling of dye adsorption onto biochars produced by thermal pyrolysis. *Journal of Water Process Engineering*, *49*, 103034.

Raza, A., Rehman, M. S. U., & Park, J. (2021). High-performance adsorption of methylene blue onto KOH-activated biochar: Influence of pH and surface functional groups. *Journal of Hazardous Materials*, *403*, 123545.

Rubangakene, N. O., Elwardany, A., Fujii, M., Sekiguchi, H., Elkady, M., & Shokry, H. (2023). Biosorption of Congo Red dye from aqueous solutions using pristine biochar and ZnO biochar from green pea peels. *Chemical Engineering Research and Design*, *189*, 636-651.

Serrano-Gómez, J., Rodríguez-Salinas, S. E., & Pérez-Cruz, M. A. (2022). pH-responsive adsorption of methylene blue onto functionalized biomass biochars. *Environmental Science and Pollution Research*, *29*, 7541–7554.

Shaban, M., Abukhadra, M. R., Khan, A. A. P., & Jibali, B. M. (2018). Removal of Congo red, methylene blue and Cr (VI) ions from water using natural serpentine. *Journal of the Taiwan Institute of Chemical Engineers*, *82*, 102-116.

Wang, J., Liu, Y., Zhang, B., & Chen, Z. (2023). Temperature-dependent adsorption behavior of dyes on biomass-derived biochar. *Bioresource Technology*, *369*, 128422. https://

Wang, Q., Chen, L., & Zheng, Y. (2022). Intraparticle diffusion and chemisorption mechanisms in dye adsorption using modified biomass-derived biochars. *Bioresource Technology*, *364*, 128058.

Weber, T. W., & Chakravorti, R. K. (1974). Pore and solid diffusion models for fixed-bed adsorbers. *AIChE Journal*, *20*(2), 228-238.

Yeboah, E., Darko, G., & Tetteh, E. K. (2023). Cocoa pod husk biochar for removal of organic dyes from wastewater: Kinetic, isotherm, and mechanistic evaluation. *SN Applied Sciences*, *5*, 312.

Zhang, Y., Li, X., & Zhou, L. (2023). Multistep diffusion-controlled adsorption of Congo red on rice husk biochar. *Journal of Environmental Chemical Engineering*, *11*(2), 109405.

Zhou, X., Wang, F., & Li, H. (2021). Adsorption kinetics of anionic dyes onto agricultural waste–derived biochars: Role of surface properties and diffusion mechanisms. *Journal of Hazardous Materials*, *420*, 126562.